AIP Applied Physics Letters

Carrier redistribution between different potential sites in semipolar (20 2 ¯ 1) InGaN quantum wells studied by near-field photoluminescence

S. Marcinkeviius, K. Gelžinyt, Y. Zhao, S. Nakamura, S. P. DenBaars, and J. S. Speck

Citation: Applied Physics Letters **105**, 111108 (2014); doi: 10.1063/1.4896034
View online: http://dx.doi.org/10.1063/1.4896034
View Table of Contents: http://scitation.aip.org/content/aip/journal/apl/105/11?ver=pdfcov
Published by the AIP Publishing

Carrier redistribution between different potential sites in semipolar $(20\bar{2}1)$ InGaN quantum wells studied by near-field photoluminescence

S. Marcinkevičius,[1] K. Gelžinytė,[1,2] Y. Zhao,[3] S. Nakamura,[3] S. P. DenBaars,[3] and J. S. Speck[3]

[1]*Department of Materials and Nano Physics, KTH Royal Institute of Technology, Electrum 229, 16440 Kista, Sweden*

[2]*Institute of Applied Research, Vilnius University, Saulėtekio 9-3, 10222 Vilnius, Lithuania*

[3]*Materials Department, University of California, Santa Barbara, California 93106, USA*

(Received 30 July 2014; accepted 6 September 2014; published online 16 September 2014)

Scanning near-field photoluminescence (PL) spectroscopy at different excitation powers was applied to study nanoscale properties of carrier localization and recombination in semipolar $(20\bar{2}1)$ InGaN quantum wells (QWs) emitting in violet, blue, and green-yellow spectral regions. With increased excitation power, an untypical PL peak energy shift to lower energies was observed. The shift was attributed to carrier density dependent carrier redistribution between nm-scale sites of different potentials. Near-field PL scans showed that in $(20\bar{2}1)$ QWs the in-plane carrier diffusion is modest, and the recombination properties are uniform, which is advantageous for photonic applications. © *2014 AIP Publishing LLC*. [http://dx.doi.org/10.1063/1.4896034]

Among $In_xGa_{1-x}N$/GaN quantum wells (QWs) of different crystallographic configurations aimed at light emission applications, semipolar $(20\bar{2}1)$ plane QWs stand out because of a high rate of In incorporation,[1,2] a good spatial uniformity of light emission,[3] and a relatively narrow linewidth.[4] This has allowed fabrication of $(20\bar{2}1)$ QW based light emitting diodes (LEDs) and lasers.[3–6] Still, efficiency of the reported devices is not optimal. To understand intrinsic limitations and develop ways of further improvement of $(20\bar{2}1)$ InGaN QW devices, especially those operating in the green spectral region, a number of material related issues remain to be solved.

Among such issues is a detailed understanding of band potential fluctuations and features of carrier recombination, and relation between them. For instance, carrier localization at band potential fluctuations in *c*-plane blue-emitting InGaN QWs has been found to isolate carriers from dislocations, resulting in decrease of the nonradiative recombination.[7,8] However, carrier localization may also have a detrimental effect by inducing current crowding and premature device degradation.[9] In other cases, regions with a lower band gap may be more defect rich and have an increased rate of the nonradiative recombination.[8,10] Even in QWs of the same crystallographic orientation and embedded into the same structure, these properties may by fundamentally different for different QW alloy compositions.[8]

Properties of carrier localization and recombination in ternary nitride QWs are often studied by photoluminescence (PL) at different temperatures and excitation power densities. Temperature dependence of PL spectra allows assessment of average localization potentials.[11] Excitation power dependence of PL intensity helps evaluation of different recombination mechanisms.[12,13] It is also a useful technique to study intrinsic electric fields in QWs induced by the difference of spontaneous and piezoelectric polarizations of QW and barrier materials.[14,15]

In most cases, such experiments are performed using standard far-field measurement techniques. The excitation spot size is usually much larger than typical dimensions of band potential fluctuations and carrier diffusion length. Therefore, such measurements provide averaged information and are inherently unable to directly determine local properties of localization and recombination. Such detailed information becomes accessible with scanning near-field optical microscopy (SNOM) where dimensions of the probed area are below the diffraction limit. Besides, scanning near-field PL measurements produce thousands of spectra and allow determination of statistical parameters that provide much richer information compared to standard PL experiments. Near-field PL has been used to study interplay between extended and localized states and local properties of recombination,[7,8,10,16–20] inhomogeneous electric field screening,[21] and spatial variations of optical polarization.[22] Near-field PL scans performed at different photoexcited carrier densities would add yet another dimension to possibilities of near-field investigations. So far, such an experimental approach has been applied in just a few occasions. Near-field PL measurements at different excitation powers were reported for polar InGaN QWs, where a PL peak shift to higher energies with increased power was observed and attributed to filling of the deep localized states.[17,20] A similar blue shift due to filling of the deep states was also detected in *m*-plane QWs, described in Ref. 23. Several works reported spectral changes induced by increased current in near-field electroluminescence (EL) of nitride LEDs.[24–26] However, EL experiments are different from PL because of a wide area, as opposed to a ~100 nm size spot, carrier injection.

In this work, near-field PL dependence on excitation power is used to study properties of carrier localization and recombination in $(20\bar{2}1)$ plane InGaN QWs. To make this study more general, we choose QWs with a broad alloy composition variation emitting from violet to green-yellow. The experimental data reveal relations between band gap fluctuations and recombination properties and allow assessing lateral transport effects taking place in these QWs.

The QW structures were grown by metal organic chemical vapor deposition on low ($\sim 10^6\,cm^{-2}$) dislocation density bulk $(20\bar{2}1)$ plane GaN substrates, provided by Mitsubishi Chemical Corporation. The structures consisted of a 1 μm undoped GaN template layer, a 3 nm thick $In_xGa_{1-x}N$ single QW, and a thin 10 nm GaN cap layer. Most of the data were obtained for QWs with nominal InN molar fractions of 0.11, 0.25, and 0.35. Some additional measurements were performed on $In_{0.31}Ga_{0.69}N$ QW.

Near-field PL measurements were carried out at room temperature with a SNOM apparatus operating in the illumination-collection (I-C) mode. In this mode, PL is excited and collected through the probe. Aluminum-coated UV fiber probes with 100 nm aperture diameter were used. Carriers were photoexcited directly into the QWs by 200 fs pulses from a frequency doubled Ti: sapphire laser with a 380 nm central wavelength and an 80 MHz pulse repetition rate. PL was measured in a time-integrated mode with a spectrometer equipped with a liquid nitrogen cooled CCD detector. Peak photoexcited carrier densities, evaluated from average excitation power densities (3 to 300 μW), probe throughput, aperture diameter, and InGaN absorption coefficient, were between 1×10^{10} and $1 \times 10^{12}\,cm^{-2}$. One should note that due to uncertainty in the probe throughput, the estimated carrier concentration may differ from the actual one by several times. The relative peak carrier densities between different measurements, however, are accurate.

Figure 1 presents typical near-field PL spectra for the violet, blue, and green-yellow emitting QWs. Figure 2 shows peak wavelength and peak intensity maps for $x = 0.35$ QW for low and high excitation powers. One can notice that wavelength and intensity spans are rather small, i.e., light emission is spatially quite uniform. Islands with similar spectral parameter values are large, extending for several μm. No small, 100-nm scale features have been observed, even for probe apertures of 50 nm and small scan steps. This is common for all the studied $(20\bar{2}1)$ QW samples in the composition range of $0.11 \leq x \geq 0.35$ and is different from an earlier study of $(20\bar{2}1)$ $In_{0.30}Ga_{0.70}N$ QW[16] that showed large amplitude and small scale ($\sim$100 nm) PL intensity and central wavelength variations, which were assigned to properties of

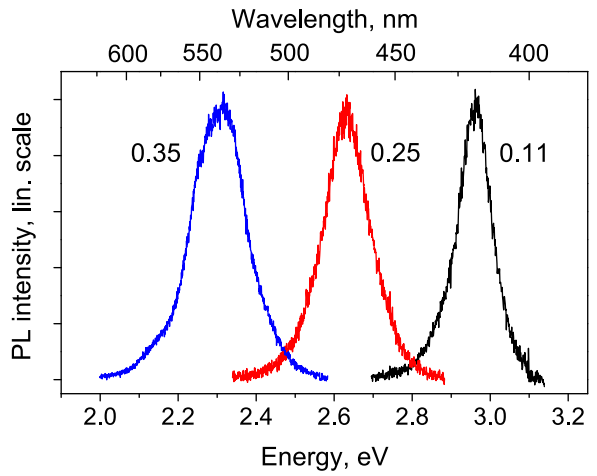

FIG. 1. Near-field PL spectra for InGaN QWs with 0.11, 0.25, and 0.35 InN molar fractions.

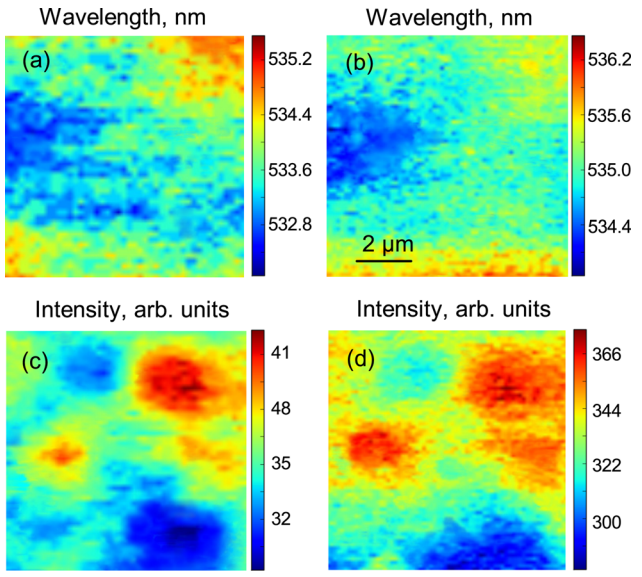

FIG. 2. $In_{0.35}Ga_{0.65}N$ QW peak wavelength (a), (b) and peak intensity (c), (d) maps for lower (10 μW) (a), (c) and higher (100 μW) (b), (d) average excitation powers.

surface morphology. Apparently, the lack of the small-scale variations and more uniform PL spectra in our QWs is a result of an optimized growth.

With increased excitation power, the peak wavelength values shift to longer wavelengths and their variation decreases. This is illustrated in Fig. 3(a) that displays a histogram of peak wavelengths for low and high excitation powers for $x = 0.35$ QW sample. Figure 3(b) shows excitation power dependence of peak wavelength standard deviation for the three samples. With excitation, the spectra become narrower, especially for the higher In content QWs, as shown in Fig. 3(c).

Excitation power dependence of average PL peak energies is shown in Fig. 4. For $x = 0.25$ and $x = 0.35$ QWs, the energy values experience a red shift. For the low In content QW ($x = 0.11$), the peak energy shows no such dependence. The peak energy shift to lower energies is quite remarkable since it is opposite to all previous far- and near-field PL observations for nitride QWs. One should note, however, that the energy shifts are small, about 10 meV, which constitutes only 6%–7% of the FWHM. Nevertheless, these changes allow to get a detailed insight into effects, taking place with increased carrier density, and provide a better understanding on carrier redistribution between different sites in $(20\bar{2}1)$ QWs.

In general, the shift of the average PL peak energy may be caused by a number of effects. These include local screening of the intrinsic electric field, band filling, spatial variations of recombination, and carrier transport effects. Let us discuss how these effects influence the carrier density dependence of the average PL peak energy and compare it to the experimental data.

The local electric field screening, as observed in SNOM experiments on *c*-plane AlGaN QWs,[21] induces a blue shift of the PL peak energy. This is contrary to our measurement results, where a red shift is observed. The band filling effect would also cause a blue shift, besides it would be similar for

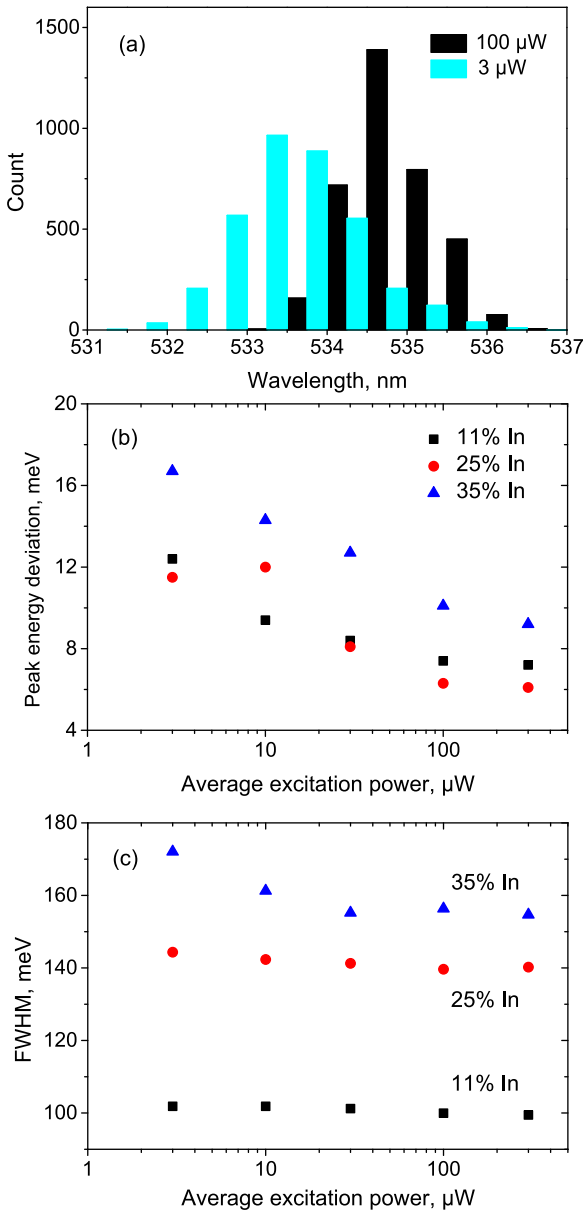

FIG. 3. Histogram of peak wavelength values for $x = 0.35$ In QW for low and high excitation powers (a). Average excitation power dependence of peak energy standard deviation (b) and FWHM (c).

QWs with different alloy compositions. No spectral shift observed for the $x = 0.11$ QW shows that the band filling, as well as the band gap shrinkage due to sample heating, is negligible in our experiments.

A red average PL energy shift with increased excitation power would require a disproportional increase of PL intensity at the low energy part of the spectra. This emission would originate from lower potential sites. At room temperature, the prevailing recombination mechanism in semipolar QWs is nonradiative.[27] For such a case, the time-integrated PL is proportional to the peak carrier concentration and the carrier lifetime. Thus, to understand the red shift, spatial carrier density and lifetime variations, and their dependence on excitation power have to be examined.

First, let us discuss transport effects. In the I-C mode, a PL spectrum is generated by carriers that, under their lifetime, remain under the probe aperture. Thus, near-field PL would be affected by carrier diffusion out of the probe area and carrier redistribution between different potential sites under the probe. Either of these effects could cause a red PL peak shift with increased excitation. The transport out of the aperture area would be more efficient for carriers generated at the higher potential sites, thus, a time-integrated PL spectrum would have a larger contribution from less mobile carriers excited in the lower potential regions. With increased excitation power (and photoexcited carrier density) such transport would increase because of the increased diffusion,[28] which would produce a PL red shift.

The relevance of this mechanism can be tested by examining excitation power dependence of the integrated PL intensity and the correlation between the peak intensity and peak energy. The PL intensity dependence on excitation power for all samples is nearly linear (Fig. 5), showing that carrier diffusion from under the probe is not efficient. Besides, a difference of diffusion efficiency for carriers in higher and lower potential sites and its increase with carrier concentration would lead to an increasingly negative correlation between the PL intensity and peak energy. The experimental data for Pearson product-moment correlation coefficient r are shown in Fig. 5. The coefficient values are small and experience a little change with power. This confirms that the large scale (>100 nm) carrier diffusion from under the probe aperture leading to their redistribution

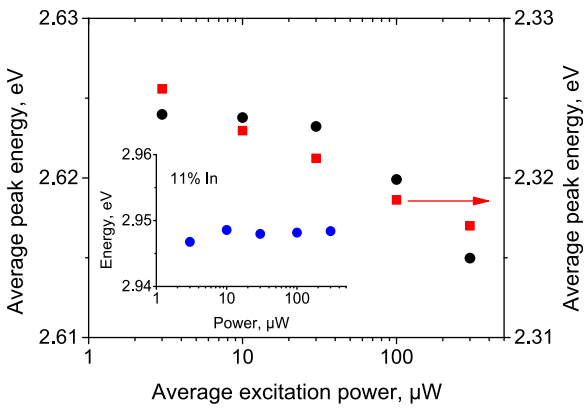

FIG. 4. Average PL peak energy dependence on excitation power for 11% In (inset), 25% In, and 35% In (right scale) QWs.

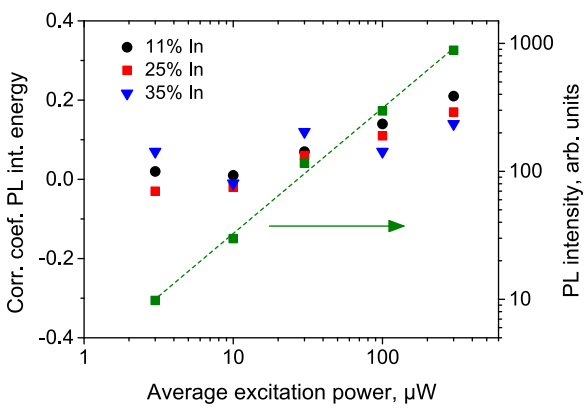

FIG. 5. Dependences of PL peak intensity—peak energy correlation coefficient and integrated PL intensity for $In_{0.35}Ga_{0.65}N$ QW on excitation power.

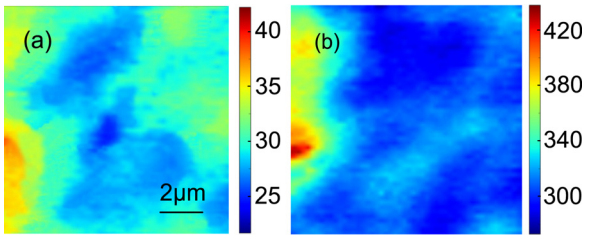

FIG. 6. Peak PL intensity maps for $In_{0.31}Ga_{0.69}N$ QW for 10 μW (a) and 100 μW (b) average excitation powers.

between microscopic higher and lower potential sites is not an efficient mechanism for the studied QWs.

Occasionally, a disproportional increase of the PL intensity at the low potential microscopic areas does occur (Fig. 6, note regions on the left). For the presented scans, the PL intensity—peak energy correlation coefficient decreases from 0.01 to −0.47 with increase of the average power from 10 to 100 μW. However, such occasions are rare and cannot be considered as a dominant effect influencing the carrier density dependent spectral changes.

Carrier redistribution between the nanoscale high and low potential regions within the probe area is a more likely effect to induce the red PL peak energy shift with power. Enhanced carrier transfer towards the lower potential sites is in accord with data of Fig. 3, which show PL peak energy red shift and the decrease of peak wavelength deviation and FWHM. An increase of carrier redistribution between different potential sites has been observed in *m*-plane QWs with increased temperature.[18] It has been attributed to enhanced carrier transfer over potential barriers separating high and low potential sites (Figs. 7(a) and 7(b)). Such barriers may form because of composition and/or strain variations; they may also occur around extended defects.[7,29] Since photoexcited carriers are hot, increased excitation would act in a similar way as temperature, increasing the mean carrier energy so that potential barriers could be traversed.[30] Alternatively, one could picture shallower and deeper localized states with the shallower ones getting filled with increased carrier density and allowing transport to the deeper ones (Figs. 7(c) and 7(d)). For different alloy compositions, the barrier heights would be different. This could explain why the nanoscale carrier transfer to the lower potential sites does not depend on the carrier density for $x = 0.11$ QW: potential barriers between the high and low potential sites in this QW might be too low to hinder the transfer even at the lowest carrier concentrations. The dissimilarity with the previous near-field PL measurements[17,20] reporting a blue shift might occur due to a larger number of low energy states in our QWs, so that the band filling does not occur. Alternatively, carrier transfer to the deep localized states in those QWs might be more efficient due to a lack of potential barriers between different potential sites (Figs. 7(e) and 7(f)).

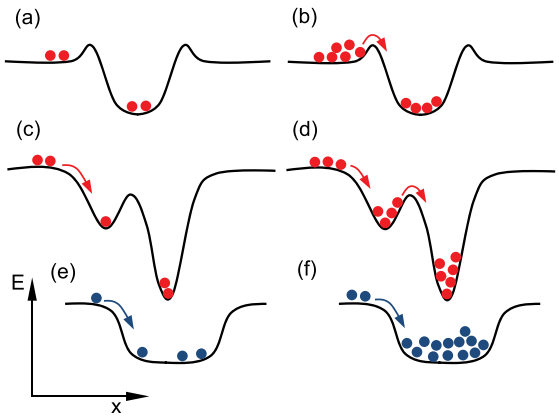

FIG. 7. Schematic diagrams of carrier transfer into deeper potential sites at low (a), (c) and high (b), (d) carrier densities over potential barriers (a), (b) and shallower localization sites (c), (d). Diagrams (e) and (f) depict low and high carrier density cases for QWs experiencing a blue shift.

For LED and laser applications, the moderate carrier redistribution different nanoscale potential sites and the negligible carrier diffusion to microscopic localization areas are advantageous, because they should contribute to wavelength stability with the driving current, prevent formation of hot spots and assure long device lifetimes. The peak wavelength and FWHM stability with current in $(20\bar{2}1)$ QW LEDs have been observed by electroluminescence experiments.[5] Recently, $(20\bar{2}1)$ QW structures showed continuous wave lasing at room temperature in the green spectral region with a threshold current of 4.3 kA/cm^2 (Ref. 31).

Finally, let us discuss a possible spatial variation of the recombination properties. At room temperature, the carrier lifetime at low and moderate carrier densities in semipolar QWs is dominated by the nonradiative recombination.[27] A red shift of the average PL peak energy with power would require a different carrier density dependence of the nonradiative recombination rates for high and low potential sites. This could occur if the nonradiative recombination centers related to the localized states would saturate, while properties of those at the extended states would not change. Such an effect, just like the carrier out-diffusion, would lead to an increase of the negative PL intensity—peak energy correlation with power, not observed in most of the scans. A weak overall correlation between the peak intensity and peak energy suggests that carrier recombination rates within the scanned area are similar. Besides, partial saturation of the nonradiative recombination centers would lead to a superlinear PL intensity dependence on the excitation power.[12,13] In the used excitation power density range, the PL intensity showed no such dependence (Fig. 5).

In conclusion, the average PL peak energy measured by SNOM in semipolar $(20\bar{2}1)$ InGaN QWs at different excitation powers was found to experience a shift to lower energies for the higher In content samples and remain independent on power for $x = 0.11$ QW. The red shift was attributed to carrier density dependent carrier redistribution between nanometer scale sites of higher and lower potentials, either due to increased transfer over potential barriers at extended and localized state interfaces or by filling shallower localized states. Overall, carrier redistribution between higher and lower potential sites was found to be modest, and recombination properties uniform, which is advantageous for photonic applications.

The research at KTH was performed within the frame of Linnaeus Excellence Center for Advanced Optics and Photonics (ADOPT) and was financially supported by the

Swedish Energy Agency (Contract No. 36652-1) and the Swedish Research Council (Contract No. 621-2013-4096). The research at UCSB was supported by the Solid State Lighting and Energy Electronic Center (SSLEEC) and by the KACST-KAUST-UCSB Solid State Lighting Program (SSLP).

[1]Y. Zhao, Q. Yan, C.-Y. Huang, S.-C. Huang, P. S. Hsu, S. Tanaka, C.-C. Pan, Y. Kawaguchi, K. Fujito, C. G. Van de Walle, J. S. Speck, S. P. DenBaars, S. Nakamura, and D. Feezell, Appl. Phys. Lett. **100**, 201108 (2012).
[2]T. Wernicke, L. Schade, C. Netzel, J. Rass, V. Hoffmann, S. Ploch, A. Knauer, M. Weyers, U. Schwarz, and M. Kneissl, Semicond. Sci. Technol. **27**, 024014 (2012).
[3]Y. Yoshizumi, M. Adachi, Y. Enya, T. Kyono, S. Tokuyama, T. Sumitomo, K. Akita, T. Ikegami, M. Ueno, K. Katayama, and T. Nakamura, Appl. Phys. Express **2**, 092101 (2009).
[4]Y. Enya, Y. Yoshizumi, T. Kyono, K. Akita, M. Ueno, M. Adachi, T. Sumitomo, S. Tokuyama, T. Ikegami, K. Katayama, and T. Nakamura, Appl. Phys. Express **2**, 082101 (2009).
[5]R. B. Chung, Y. D. Lin, I. Koslow, N. Pfaff, H. Ohta, J. Ha, S. P. DenBaars, and S. Nakamura, Jpn. J. Appl. Phys., Part 1 **49**, 070203 (2010).
[6]M. Ueno, Y. Yoshizumi, Y. Enya, T. Kyono, M. Adachi, S. Takagi, S. Tokuyama, T. Sumitomo, K. Sumyioshi, N. Saga, T. Ikegami, K. Katayama, and T. Nakamura, J. Cryst. Growth **315**, 258 (2011).
[7]F. Hitzel, G. Klewer, S. Lahmann, U. Rossow, and A. Hangleiter, Phys. Rev. B **72**, 081309(R) (2005).
[8]A. Kaneta, M. Funato, and Y. Kawakami, Phys. Rev. B **78**, 125317 (2008).
[9]A. Pinos, S. Marcinkevičius, J. Yang, Y. Bilenko, M. Shatalov, R. Gaska, and M. S. Shur, Appl. Phys. Lett. **95**, 181914 (2009).
[10]A. Pinos, V. Liuolia, S. Marcinkevičius, J. Yang, R. Gaska, and M. S. Shur, J. Appl. Phys. **109**, 113516 (2011).
[11]Y. H. Cho, G. H. Gainer, A. J. Fisher, J. J. Song, S. Keller, U. K. Mishra, and S. P. DenBaars, Appl. Phys. Lett. **73**, 1370 (1998).
[12]S. Marcinkevičius, U. Olin, and G. Treideris, J. Appl. Phys. **74**, 3587 (1993).
[13]O. Brandt, H. Yang, and K. H. Ploog, Phys. Rev. B **54**, R5215 (1996).
[14]S. Marcinkevičius, A. Pinos, K. Liu, D. Veksler, M. S. Shur, J. Zhang, and R. Gaska, Appl. Phys. Lett. **90**, 081914 (2007).
[15]A. Pinos, S. Marcinkevičius, K. Liu, M. S. Shur, E. Kuokštis, G. Tamulaitis, R. Gaska, J. Yang, and W. Sun, Appl. Phys. Lett. **92**, 061907 (2008).
[16]A. Kaneta, Y.-S. Kim, M. Funato, Y. Kawakami, Y. Enya, T. Kyono, M. Ueno, and T. Nakamura, Appl. Phys. Express **5**, 102104 (2012).
[17]A. Kaneta, K. Okamoto, Y. Kawakami, S. Fujita, G. Marutsuki, Y. Narukawa, and T. Mukai, Appl. Phys. Lett. **81**, 4353 (2002).
[18]S. Marcinkevičius, K. M. Kelchner, S. Nakamura, S. P. DenBaars, and J. S. Speck, Appl. Phys. Lett. **102**, 101102 (2013).
[19]S. Marcinkevičius, Y. Zhao, K. M. Kelchner, S. Nakamura, S. P. DenBaars, and J. S. Speck, Appl. Phys. Lett. **103**, 131116 (2013).
[20]A. Vertikov, A. V. Nurmikko, K. Doverspike, G. Bulman, and J. Edmond, Appl. Phys. Lett. **73**, 493 (1998).
[21]H. Murotani, T. Saito, N. Kato, Y. Yamada, T. Taguchi, A. Ishibashi, Y. Kawaguchi, and T. Yokogawa, Appl. Phys. Lett. **91**, 231910 (2007).
[22]R. Micheletto, M. Allegrini, and Y. Kawakami, Appl. Phys. Lett. **95**, 211904 (2009).
[23]V. Liuolia, A. Pinos, S. Marcinkevičius, Y. D. Lin, H. Ohta, S. P. DenBaars, and S. Nakamura, Appl. Phys. Lett. **97**, 151106 (2010).
[24]J. Christen, T. Riemann, F. Bertram, D. Rudloff, P. Fischer, A. Kaschner, U. Haboeck, A. Hoffmann, and C. Thomsen, Phys. Status Solidi C **0**, 1795 (2003).
[25]H. Itoh, S. Watanabe, M. Goto, N. Yamada, M. Misra, A. Y. Kim, and S. A. Stockman, Jpn. J. Appl. Phys., Part 2 **42**, L1244 (2003).
[26]A. Pinos, S. Marcinkevičius, J. Yang, R. Gaska, M. Shatalov, and M. S. Shur, J. Appl. Phys. **108**, 093113 (2010).
[27]S. Marcinkevičius, R. Ivanov, Y. Zhao, S. Nakamura, S. P. DenBaars, and J. S. Speck, Appl. Phys. Lett. **104**, 111113 (2014).
[28]R. Aleksiejūnas, K. Gelžinytė, S. Nargelas, K. Jarašiūnas, M. Vengris, A. Armour, D. P. Byrnes, R. A. Arif, S. M. Lee, and G. D. Papasouliotis, Appl. Phys. Lett. **104**, 022114 (2014).
[29]A. Mouti, J.-L. Rouvière, M. Cantoni, J.-F. Carlin, E. Feltin, N. Grandjean, and P. Stadelmann, Phys. Rev. B **83**, 195309 (2011).
[30]S. Marcinkevičius and R. Leon, Appl. Phys. Lett. **76**, 2406 (2000).
[31]M. Adachi, Y. Yoshizumi, Y. Enya, T. Kyono, T. Sumitomo, S. Tokuyama, S. Takagi, K. Sumiyoshi, N. Saga, T. Ikegami, M. Ueno, K. Katayama, and T. Nakamura, Appl. Phys. Express **3**, 121001 (2010).